Time variant spectral inversion

Alana R. Schoepp and Gary F. Margrave

ABSTRACT

Nonstationary filtering techniques can be used to create nonstationary deconvolution operators designed directly from the seismic data and apply them to the data. Such operators can be continuously time-variant and have any desired amplitude and phase spectra. The operator design uses time-variant Fourier or Burg spectra measured directly from seismic data, which are smoothed, inverted, and combined with a minimum-phase spectrum, if desired. This method of deconvolution, named time-variant spectral inversion (TVSI), approximately corrects the seismic data for the effects of anelastic attenuation, frequency dispersion, and source signature. The result is a one-dimensional nonstationary operation which extends the range of stationary deconvolution to a type of data-driven inverse-Q filter.

INTRODUCTION

As a wave propagates through an anelastic medium, some of its energy becomes converted to heat by the internal friction of the medium and is irreversibly lost. The amount of energy loss due to absorption is an intrinsic property of an anelastic medium and is commonly described by the dimensionless parameter, Q. The quality factor, Q, is also referred to as the internal friction or dissipation factor. Although there are several different equations used to describe Q (see Johnston and Toksov, 1981, for a description), the most common is that Q is the ratio of the stored energy to the dissipated energy in a wave:

$$Q=-2\pi E/\Delta E, \tag{1}$$

where E is the elastic energy and - ΔE is the energy loss per cycle of the wave. The constant Q theory (Kjartansson, 1979) postulates that Q is independent of frequency over the range of seismic frequencies and experimental evidence supports this as well.

In practice it can be difficult to isolate the effects of anelastic attenuation described by Q from the effects of other attenuative mechanisms. Transmission losses, geometrical spreading (spherical divergence), mode conversion, intrabed multiples and scattering of acoustic energy all contribute to the degradation of seismic signal (Schoenberger and Levin, 1974). Time-variant spectral inversion, as presented in this paper cannot distinguish the effects of Q from the effects of stratigraphic filtering.

Absorption is necessarily accompanied by minimum phase dispersion in a linear, causal medium (Futterman, 1962). Therefore, since a causal pulse in a linear absorbing medium is minimum phase, its phase spectrum is related to the log of its amplitude spectrum by the Hilbert transform (Karl, 1989).

Absorption makes all seismic data nonstationary. “Nonstationary” is a general term used to describe a property that is variant with time or space. In contrast, stationary refers to a property that is invariant. In practical applications, the term nonstationary is meaningful only when used in reference to a measure. For example a time series of reflection coefficients fluctuates randomly corresponding to geology. On a small scale, these fluctuations of the reflection coefficients could be described as nonstationary, however we may choose to describe the reflectivity as stationary because large scale averages are not systematically changing. The term nonstationary can used to describe a property that is time-variant and in the context of this work, the two words are interchangeable. This paper describes a specific application, a time-variant inverse or deconvolution filter, based on the more general nonstationary filter theory.

The essence of Q theory is that anelastic losses are time and frequency dependent and therefore spectral attenuation and amplitude (time-domain) decay are two manifestations of the same problem. Absorption causes a seismic pulse to broaden and decrease in amplitude in the time domain while losing spectral bandwidth in the frequency domain. Figure 1 shows the effects of anelastic attenuation corresponding to Q of 50, on a minimum phase wavelet versus traveltime. Conventional stationary methods to improve resolution of seismic data include deconvolution and frequency-independent gain. These methods attempt to separate time-domain effects from frequency-domain effects and treat both problems individually. Gain is applied to boost the amplitude of temporal events at later times, and conventional stationary deconvolution is designed to remove the source signature and recover lost high frequencies in an effort to restore resolution.

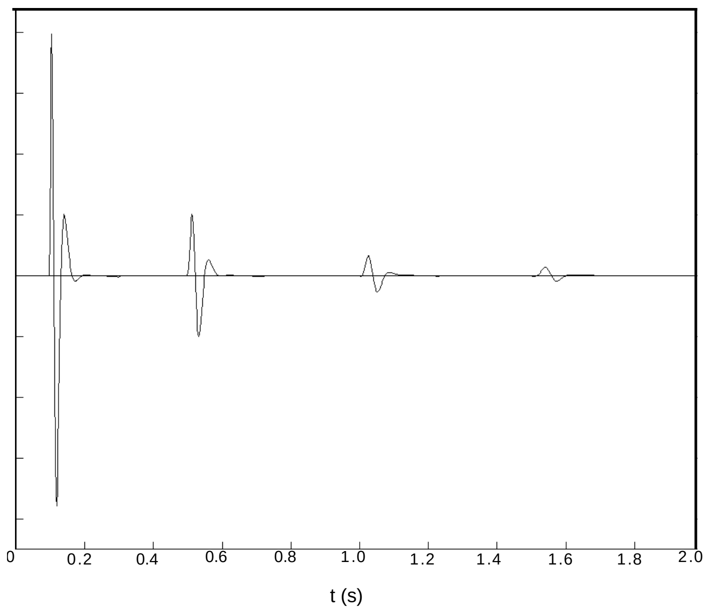

Figure 1: A pulse traveling through a one-dimensional anelastic medium, Q=50, broadens and its amplitude decreases with time.

The purpose of time-variant spectral inversion (TVSI) is to correct for time and frequency-domain effects simultaneously, in accordance with our understanding of how earth processes created these effects in the data. TVSI has been developed from a model of a wavelet propagating through the earth which suffers frequency-dependent attenuation and dispersion along its travelpath. TVSI removes the time and frequency domain effects of attenuation as well as the effects of source signature thereby increasing resolution and boosting the amplitude of events at later times. In a lossless medium ($Q \rightarrow \infty$) the propagating wavelet is time-invariant and the nonstationary deconvolution (TVSI) process becomes stationary deconvolution and only removes the source signature. TVSI can be considered as a data-driven inverse-Q filter.

Other inverse-Q filtering algorithms have been developed. Hale (1982) proposes an inverse-Q filter and deconvolution called Q Adaptive Deconvolution. This method is implemented with a prediction error filter and attempts to compensate for attenuation, dispersion, and source waveform. In addition, it yields an estimate of Q.

BACKGROUND

TVSI has been developed as an extension of the basic concepts of the stationary convolutional model and stationary deconvolution. Therefore, a review of the stationary convolutional model and stationary Fourier domain deconvolution will be presented in this section. Next, to develop TVSI from stationary deconvolution, a technique is required which will decompose a trace or operator on a time-frequency grid. For this purpose we use a time-variant spectrum (TVS), which is introduced to explicitly describe how the spectrum of a trace or operator changes with time. Once we have this method of describing a nonstationary operator, we will briefly examine how it may be applied to the data.

In the stationary convolutional model, a seismic trace is composed of the reflectivity of the earth, r(t), the near surface multiples, m(t), and the source wavelet, w(t). These factors are related together, in the time domain, through convolution to produce the seismic trace, s(t):

$$s(t) = r(t) * m(t) * w(t). \tag{2}$$

In the frequency domain, convolution becomes multiplication and the above equation becomes:

$$S(f) = R(f)M(f)W(f). \tag{3}$$

Fourier or frequency domain stationary deconvolution is based on the convolutional model and deconvolves the trace by exploiting the similarities between the power spectrum of the trace and the power spectrum of the wavelet. The power spectrum of the trace is computed and smoothed to obtain an estimate of the power spectrum of the wavelet. Since a linear, causal pulse in an absorbing medium is minimum phase (Futterman, 1962), the minimum phase spectrum of the wavelet can be calculated as the Hilbert transform of the logarithm of the amplitude spectrum. The trace is then deconvolved by dividing the trace by the estimated amplitude and phase spectrum of the wavelet.

To develop TVSI, a tool is needed to examine how the spectrum of a trace changes with time. A time-variant spectrum, TVS, is calculated from the input data by applying a window to the input trace and calculating the ordinary Fourier spectrum of the windowed data, as shown in Figure 2. The window is then moved successively down the trace and the Fourier spectrum is calculated for each new position of the window. Typically there is an overlap of 80 to 90 percent between neighboring windows. (This technique is known as the spectrogram or short time Fourier transform (Cohen, 1995)). A TVS can be displayed as a grey level plot or a 3-dimensional surface plot, with frequency as the horizontal coordinate and time as the vertical coordinate. In the grey level plots, black represents large positive numbers and light grey represents small positive numbers. Each row of the plot corresponds to the complete spectrum of the windowed input data at a specific time. In general, a TVS is complex valued and contains both amplitude and phase information. The amplitude (magnitude) of the TVS, will be referred to as |TVS|.

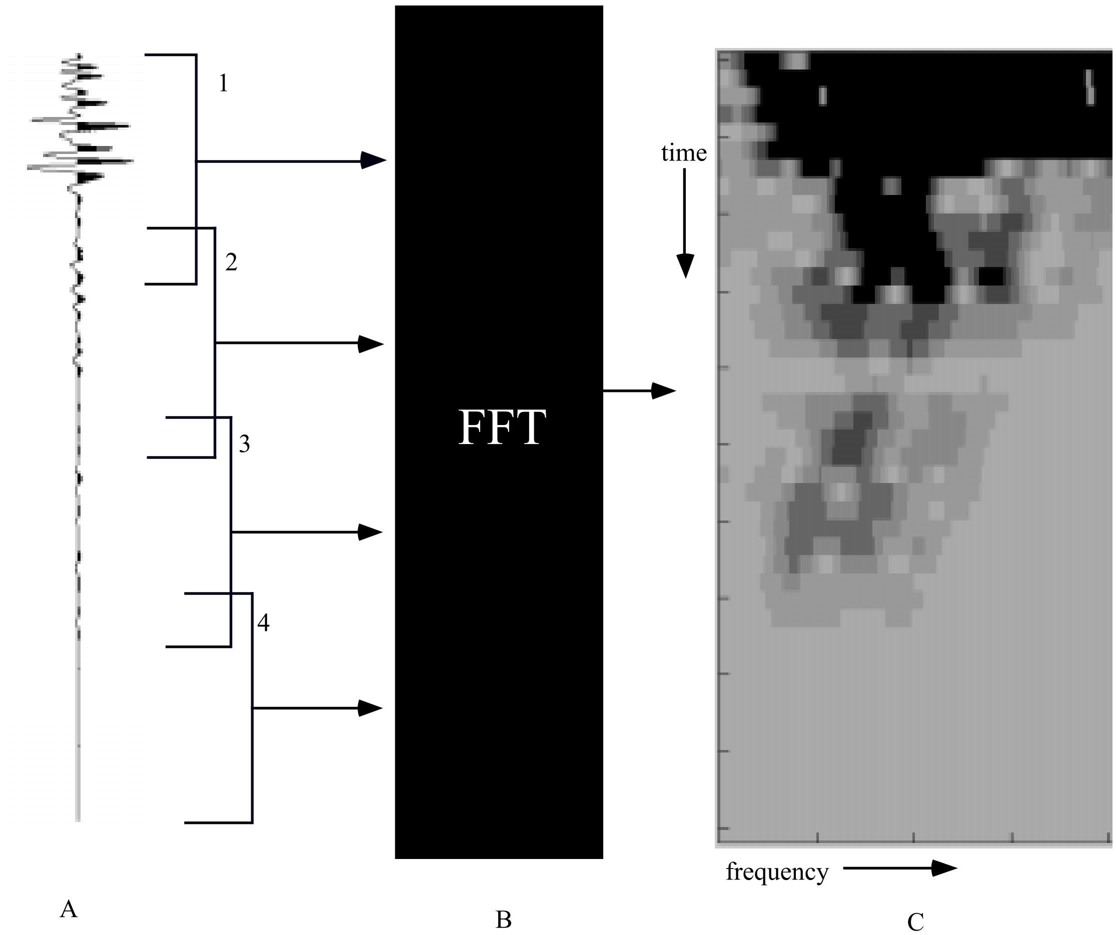

Figure 2: A window is applied to a seismic trace, as in step A, and the ordinary Fourier spectrum of the windowed data is calculated (step B). This spectrum then becomes a row of the resulting nonstationary spectrum, C. The window is then moved successively down the trace, with a large degree of overlap, and the spectrum is calculated at each new position of the window to create the nonstationary spectrum.

The relative detail in time and frequency of the TVS is related to the window size as governed by the uncertainty principle. The uncertainty principle, which may be familiar from quantum mechanics, states:

$$\Delta t \Delta f = \text{constant}, \tag{4}$$

where Δt is the window length in time and Δf is the length of the spectrum of the window in frequency. The uncertainty principle is the relationship between the widths of a Fourier transform pair in their respective domains. For example, a boxcar window in the time domain will become a sinc function in the frequency domain and the width of each is interrelated as determined by equation 4.

A seismic trace analyzed in the frequency domain, is given by:

$$G(f) = \int s(t)w(t)\, e^{-2\pi i f t}\, dt \;=\; \int S(f')\, W(f-f')df', \tag{5}$$

where s(t) is the seismic trace, and S(f) is its corresponding frequency spectrum. The window, in time, is denoted by w(t), its frequency spectrum is W(f). G(f) is the spectrum of the windowed data. Convolution is a smoothing operator, so therefore S(f) is smoothed on the scale of Δf, and the extent of this smoothing increases as Δt becomes smaller. Therefore, some consideration is required when choosing a window length parameter as it will affect the frequency resolution of the resulting TVS.

Time-variant spectra can be applied to seismic data as nonstationary operators in a manner similar to the application of stationary operators. A stationary wavelet can be applied to a reflectivity via Fourier transform techniques:

$$S(f) = W(f)\int r(t)e^{-2\pi i f t}dt, \tag{6}$$

where S(f) is the stationary spectrum of a trace, W(f) is the stationary forward operator (wavelet), and r(t) is the reflectivity in the time domain. The reflectivity in the Fourier domain is computed from the trace using the inverse operator:

$$R(f) = W^{-1}(f)\int s(t)e^{-2\pi i f t}dt, \tag{7}$$

where R(f) is the reflectivity in the Fourier domain, $W^{-1}(f)$ is the inverse of the spectrum of the wavelet, and s(t) is the trace in the time domain. The forward application of a nonstationary operator $W_p(t,f)$ can be applied to the reflectivity in a similar manner, through the following formula (Margrave, 1997):

$$S(f) = \int r(t)W_p(t,f)e^{-2\pi i f t}dt. \tag{8}$$

By hypothesis, for quasi-stationary processes, the inverse operator $W_p^{-1}(t,f)$ can be applied to the input trace by:

$$R(f) = \int S(t){W_p}^{-1}(t,f)e^{-2\pi f t}dt. \tag{9}$$

NONSTATIONARY SPECTRAL MODEL

Implicit in the creation of a spectral inverse operator is a model which relates the spectrum of the input trace to those effects which we would like to remove. The stationary convolutional model as described in equation (3) can be extended into the nonstationary realm to yield a model of the TVS, S(t,f), of an attenuated, nonstationary seismic trace:

$$S(t,f) = R(t,f)M(t,f)W(f)e^{-\pi\alpha(t,f)ft+i\phi(t,f)}, \tag{10}$$

where R(t,f) is the nonstationary TVS of the earth's reflectivity function, which we assume to be statistically white in f and stationary over large time scales. M(t,f) is the nonstationary TVS describing multiple reflections, W(f) is the stationary spectrum of the source signature including stationary near surface effects, $\alpha(t,f)$ is a generalized nonstationary attenuation function, and $\phi(t,f)$ is the phase associated with attenuation. If $\alpha=1/Q(t)$, the exponential attenuation becomes the constant Q model of attenuation. Equation (10) can also be written in terms of the amplitude spectrum of each component:

$$|S(t,f)| = |R(t,f)||M(t,f)||W(f)|e^{-\pi\alpha(t,f)ft}. \tag{11}$$

Note that if the time dependence of equation (10) vanishes, then the stationary convolutional model, equation (3), results.

From equation (11) we can see the amplitude of the forward operator, $|W_p(t,f)|$ acting on the reflectivity is modeled as:

$$|W_p(t,f)| = |M(t,f)||W(f)|e^{-\pi\alpha(t,f)ft} \qquad (12)$$

The forward operator contains the attenuation and source effects and it physically represents a wavelet propagating through the earth and attenuating with time. The forward operator can be estimated by attempting to eliminate the reflectivity, R(t,f), from equation (11). As in stationary Fourier domain deconvolution we assume that the reflectivity effects can be removed through smoothing the |TVS| of the seismic trace. It is not clear what the smoothing does to |M(t,f)|. We assume that the general trend of the TVS of the seismic trace is due to propagation effects and source waveform, and that the detail in the TVS is due to reflectivity. The forward operator can be left as zero phase or coupled with a minimum phase spectrum, which seems reasonable as we expect the earth to have minimum phase attenuative processes. The forward operator is then inverted and applied to the data using equation (9).

The assumptions that have been made to simplify the spectral inversion process limit the TVSI procedure. We assume one-dimensional wave propagation and therefore require spherical divergence corrections to be applied prior to TVSI. Also, as with stationary deconvolution, TVSI cannot correct for all multiple effects, although it can potentially handle a wider class of multiples than stationary deconvolution. For simplicity, we assume that the attenuation depends only on travel time and not raypath. The minimum phase assumption of a linear , causal earth is a simplification which can lead to phase complications. The phase computations in the TVSI algorithm are handled with a digital Hilbert transform. Since minimum-phase attenuation is created in the earth through analog means, removal of this phase through digital means is inexact.

METHOD

The first step of the TVSI algorithm is to apply an approximate and deterministic gain to the input trace. This is done to prevent aliasing of the steep decay surface when the input trace is windowed during the calculation of the TVS. The gain is a computational convenience and is removed from the resultant trace after the inversion process. Gaining the trace adjusts the amplitude of the trace exponentially in time and the |TVS| of the gained trace is given by:

$$|S(t,f)| = |R(t,f)||M(t,f)||W(f)|e^{-\pi ft/Q+\lambda t}, \qquad (13)$$

where λ is a gain constant.

We have investigated two methods to attempt to eliminate reflectivity from the above |TVS| to obtain the forward operator. The first method is simple-smoothing and the second is residual-smoothing. In the simple smoothing method, the |TVS| of the input trace is smoothed directly in both time and frequency. An ideal smoother B(t,f) will have the property:

$$|\overline{R(t,f)}| = |R(t,f)| ** B(t,f) \approx 1, \qquad (14)$$

where $|\overline{R(t,f)}|$ is the |TVS| of the smoothed reflection coefficients, B(t,f) is an appropriate smoother, and ** denotes two-dimensional convolution. This smoother is then applied to equation (11) to reveal the forward operator:

$$|W_p(t,f)| = B(t,f) ** |S(t,f)| = B(t,f) ** (|R(t,f)||M(t,f)||W(f)| e^{-\pi ft/Q+\lambda t}), \quad (15)$$

$$|W_p(t,f)| \approx |M(t,f)||W(f)| e^{-\pi ft/Q+\lambda t}. \quad (16)$$

We note that equation (16) does not follow mathematically, but is an assumption consistent with standard practice in stationary deconvolution.

A smoother applied to the |TVS| of equation (11) , as described in equation (14), will act on the multiples, M(t,f), the source waveform, W(f), and the attenuation/gain surface, $e^{-2\pi ft+\lambda t}$, as well as the reflection coefficients. The source waveform is assumed to be time-invariant, so a time smoother should not affect it. However, the attenuation/gain surface is very steep, as it is exponential in both time and frequency. A smoother applied to this surface will reduce its slope. Therefore when the final filter is inverted and applied, the exponential decay surface will not be completely removed from the input trace.

To address the smoothing issues mentioned above and reduce the bias introduced by smoothing the exponential-decay/gain surface, a second smoothing method was devised as an alternative to the simple-smoothing method. The residual-smoothing method explicitly models the attenuation as an exponential surface in frequency and time whose shape is determined by the quality factor, Q (assumed to be the constant Q model). Assuming that an estimate of Q, $\hat{Q}$, is available and setting multiple effects to unity. The attenuation/gain surface can be removed approximately from the |TVS| of equation (13) to produce a residual spectrum:

$$|\rho(t,f)| = |R(t,f)||W(f)| e^{-\pi ft/Q+\lambda t} e^{\pi ft/\hat{Q}-\lambda t} \quad (17)$$

$$|\rho(t,f)| = |R(t,f)||W(f)| e^{\pi ft(-Q^{-1}+\hat{Q}^{-1})} \approx |R(t,f)||W(f)|. \quad (18)$$

The residual spectrum, $|\rho(t,f)|$, is mostly free from attenuation effects and is dominated by the spectra of the source signature and reflectivity. The general trend of the residual spectrum is thought to be due to the source signature and the detail in the spectrum is from the reflectivity. This residual spectrum is then smoothed two-dimensionally with time and frequency smoothers to remove the reflectivity from the residual spectrum:

$$|\overline{\rho(t,f)}| = B(t,f) ** |\rho(t,f)| \approx B(t,f) ** (|R(t,f)||W(f)|), \quad (19)$$

$$|\overline{\rho(t,f)}| \approx |W(f)|, \quad (20)$$

where $|\overline{\rho(t,f)}|$ is the |TVS| of the smoothed residual spectrum, $|\rho(t,f)|$ is the |TVS| of the unsmoothed residual, and B(t,f) is an appropriate smoother. Equation (20) also follows by assumption and not strictly mathematically. The reflectivity coefficients are assumed to be white and the smoother satisfies equation (13). In this manner, the reflectivity effects can be removed from the |TVS| without overly biasing the attenuation effects. Figure 3 illustrates the TVSI process up to this point by showing the |TVS| of the ungained input trace, gained input trace and the smoothed residual spectrum.

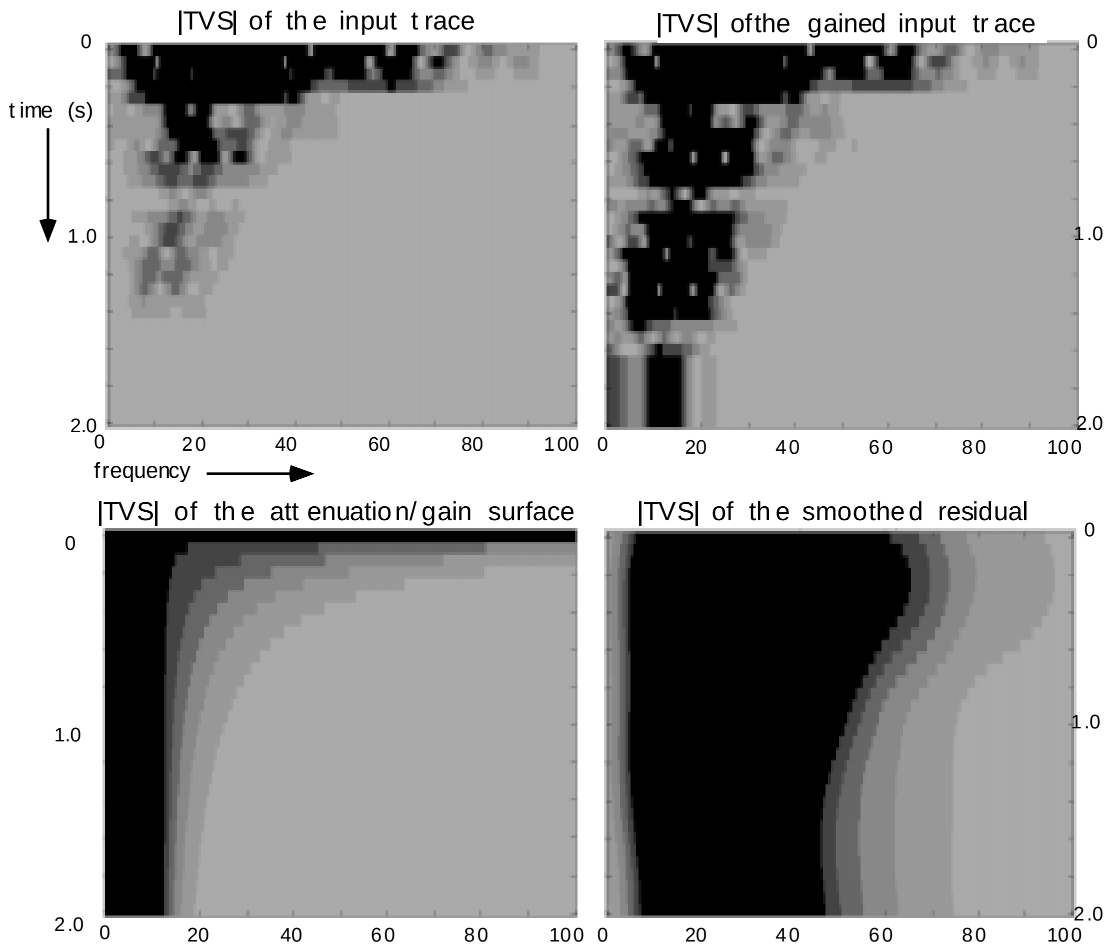

Figure 3: The |TVS| of the input trace is shown in 3A. The trace is initially gained and the |TVS| of the gained input trace is shown in 3B. The |TVS| of an attenuation/gain surface can be calculated and divided from the |TVS| of the gained input trace. This residual |TVS| is then smoothed, and the result is shown as 3D.

After the smoothing process, the attenuation spectrum is restored to the smoothed residual spectrum to yield an estimate of the propagating wavelet with gain applied:

$$|\overline{W_p(t,f)}| \approx |\overline{\rho(t,f)}|\, e^{-\pi f t / Q + \lambda t} \quad . \tag{21}$$

The operator may be left as zero phase or combined with a minimum phase spectrum. The minimum phase spectrum is calculated as prescribed from the following equation:

$$\phi_{min}(t,f)=H(\ln(W_p(t,f)+n)), \tag{22}$$

where ϕ_{min} is the nonstationary minimum phase spectrum, H is a one-dimensional Hilbert transform over frequency at constant time, $W_p(t,f)$ is the amplitude spectrum of the forward operator, and n is a small amount of noise.

The |TVS| of the propagating wavelet can be inverted to produce the inverse operator:

$$| W_p(t,f) |^{-1} \approx | \overline{\rho(t,f)} | \, e^{\pi f t / Q - \lambda t + \phi(t,f)} \tag{23}$$

The forward operator ,$|W_p(t,f)|^{-1}$, is then applied to the trace to remove the, attenuation, source signature and imposed gain to give an estimate of the reflectivity. Figure 4 shows the |TVS| of the propagating wavelet, the |TVS| of the propagating wavelet with gain applied, and the |TVS| of the inverse operator.

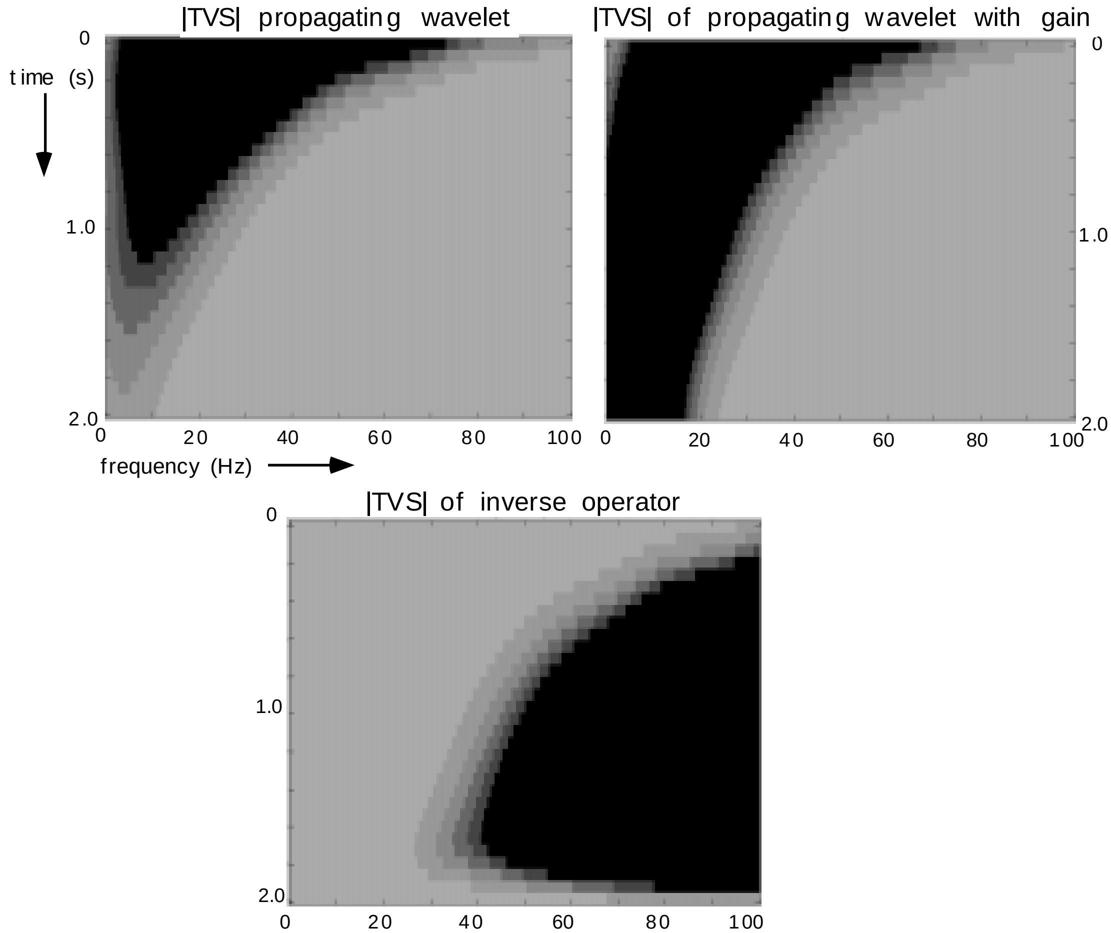

Figure 4: The |TVS| of the propagating wavelet is shown in 4A. The propagating wavelet with gain applied (4B), is then inverted to form the |TVS| of the inverse operator, 4C.

RESULTS

Results from applying TVSI to a noise-free and multiple-free synthetic will be presented. The synthetic trace was created by applying a Q filter (Q=25) superimposed with a minimum-phase wavelet to a reflectivity time series. First, the results from the four possible versions of TVSI (simple smoothing and residual-smoothing with both zero and minimum-phase operators) are compared to the results from stationary deconvolution algorithms. Next the smoothing parameters are examined to see how they affect the output trace of TVSI. Finally, the residual-smoothing version is tested for its sensitivity to errors in the estimate of Q.

Figure 5 shows the results from all versions of TVSI (minimum-phase and zero-phase, simple-smoothing and residual-smoothing) and compares them to the input trace, bandlimited reflectivity, and results from time-variant spectral whitening (TVSW), gain and Wiener deconvolution, and gain and stationary frequency domain deconvolution. Time variant spectral whitening (Yilmaz, 1987) is a zero-phase technique to compensate seismic data for attenuation. The bandlimited reflectivity represents the ideal output trace. Figures 6 and 7 display the |TVS| of the traces in figure 5.

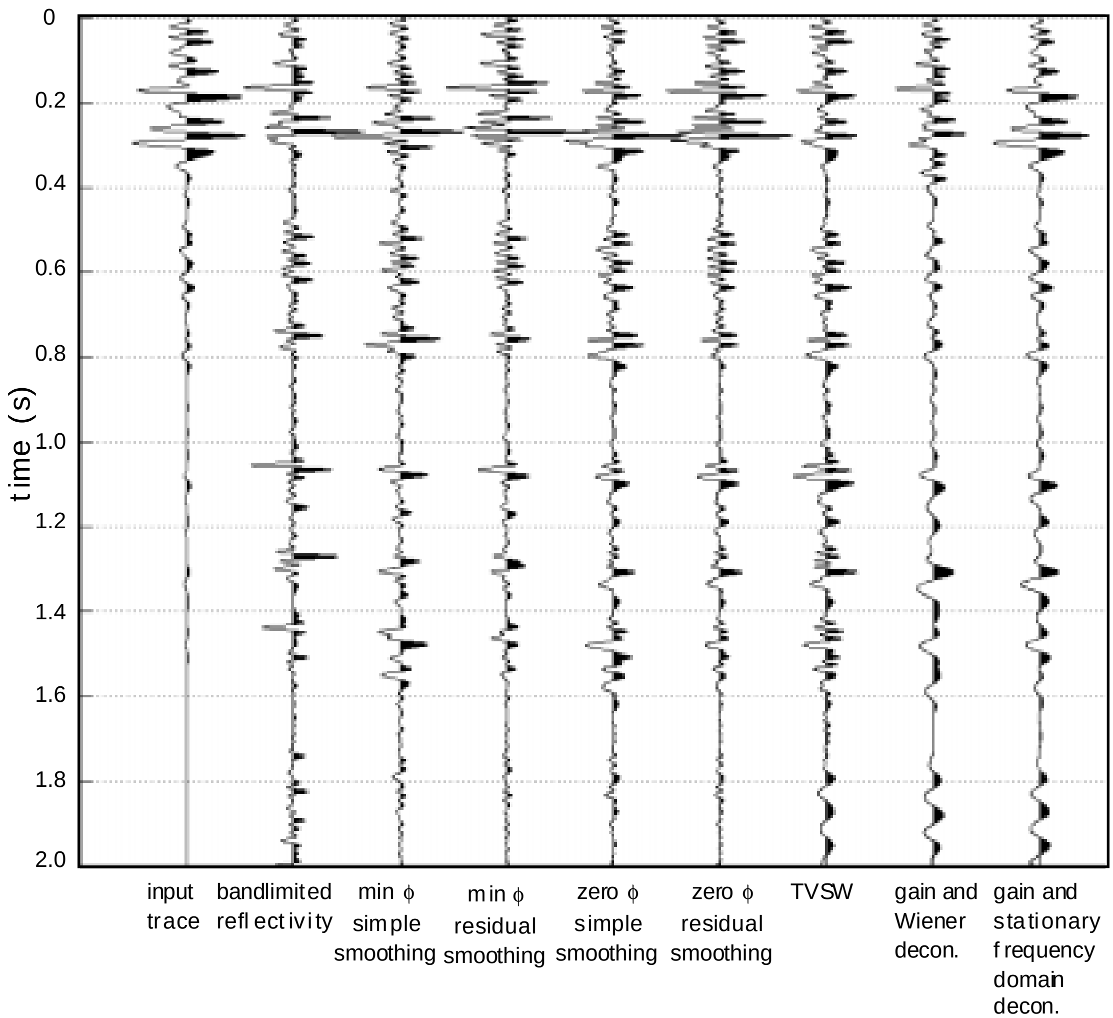

Figure 5: A comparison of various deconvolution techniques. The four combinations of TVSI are displayed next to each other. The operators in the simple-smoothing version were smoothed with 10 Hz frequency smoothers and 0.1 second time smoothers. The operators in the residual-smoothing version were smoothed with 10 Hz frequency smoothers and 1.5 second time smoothers. In TVSI, a stabilization factor of 0.001 (the fraction of the maximum value of the matrix) was added before inversion of the attenuation/gain surface and before inversion of the operator. The Wiener operator was designed on the first 0.3 seconds of the input trace and 50 autocorrelation lags were used in the operator design. The smoother in the stationary frequency domain deconvolution was 30 points in length. Both stationary deconvolution methods had a stabilization factor of 0.0001 (the fraction of the zero lag of the autocorrelation) added as white noise before inversion of the operator.

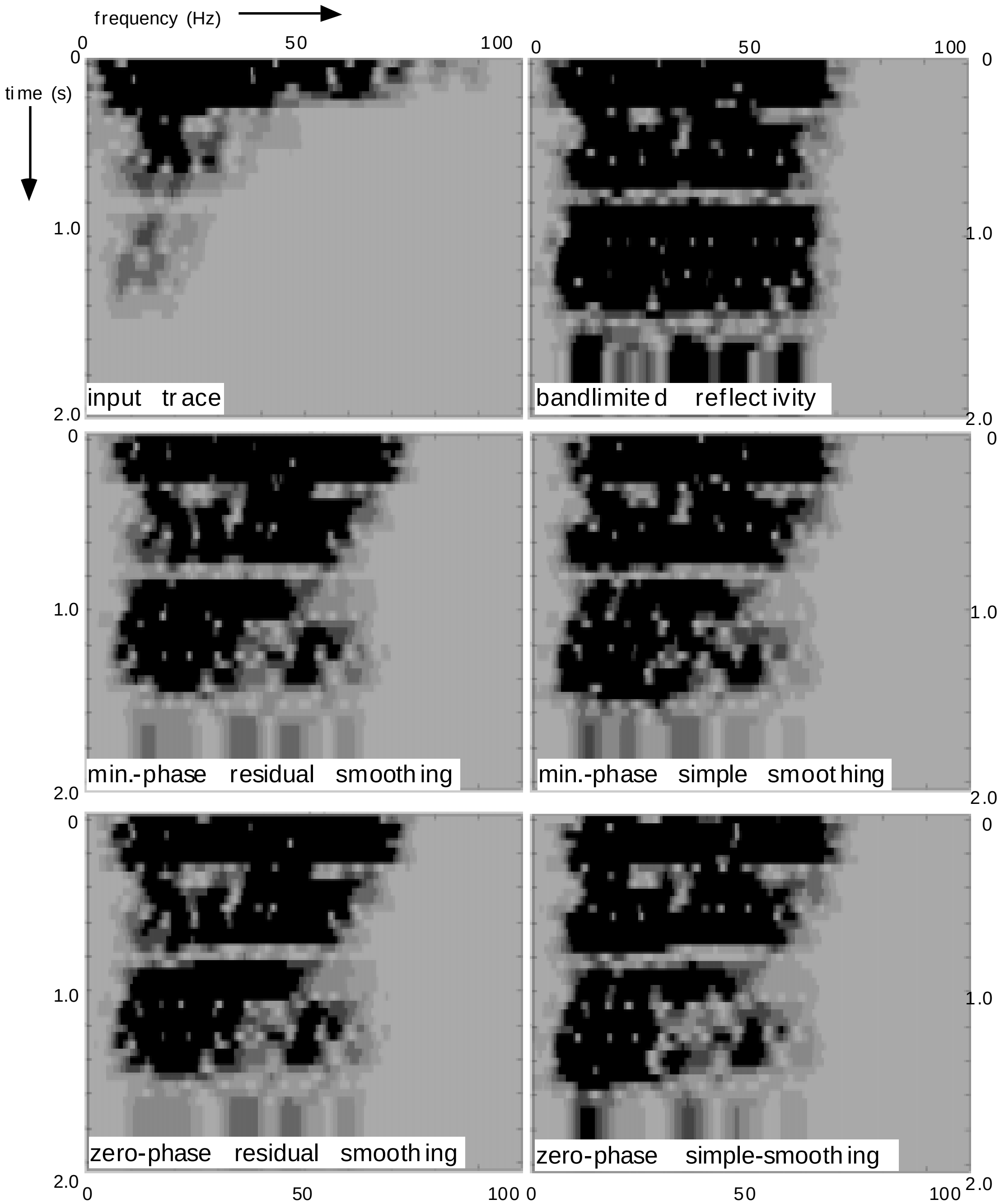

Figure 6: A comparison of the |TVS| of the output trace from the residual-smoothing and the simple-smoothing method, in both minimum and zero phase.

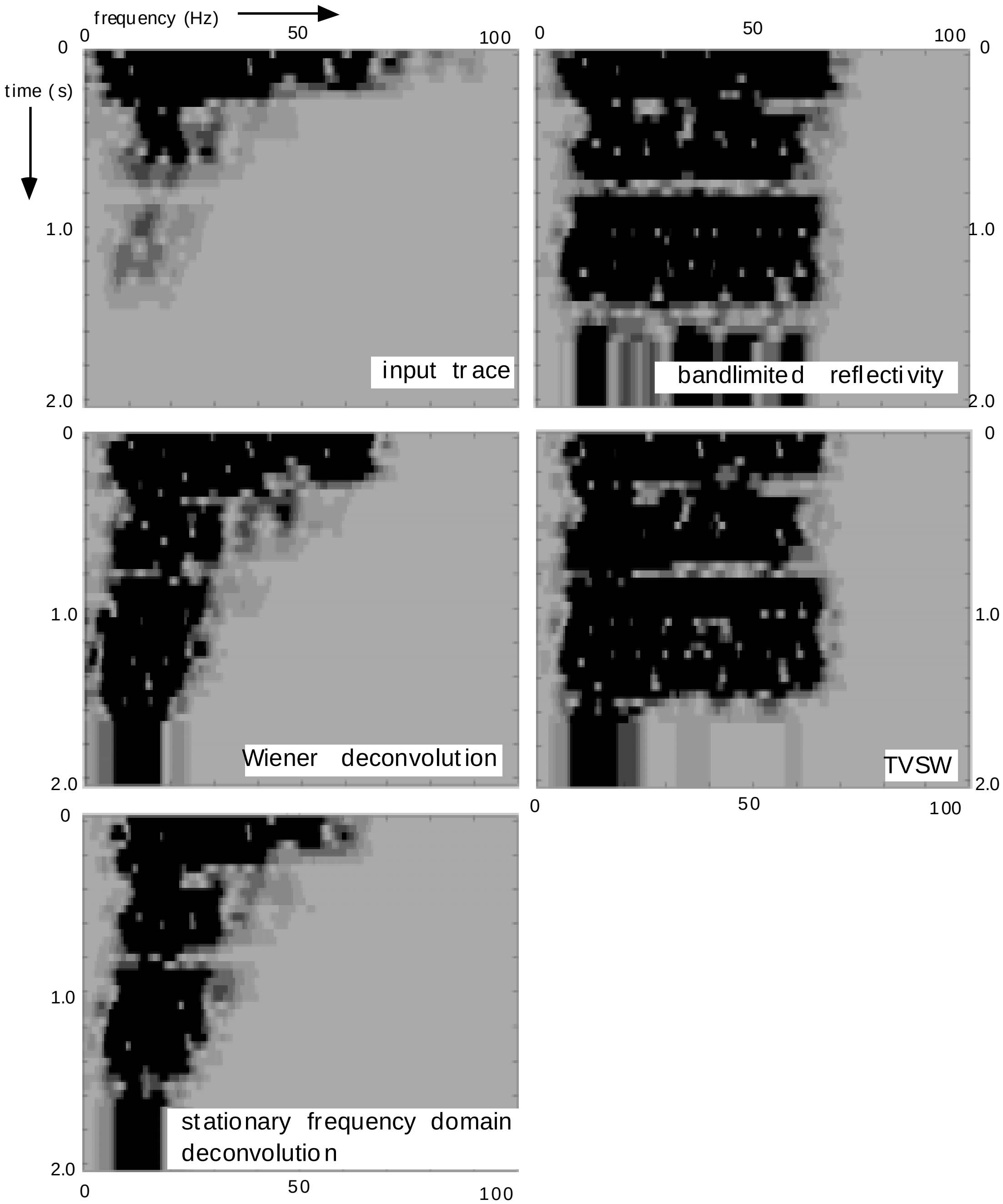

Figure 7: A comparison of the |TVS| of the results from the combination of gain and Wiener deconvolution, TVSW, and gain and stationary frequency domain deconvolution.

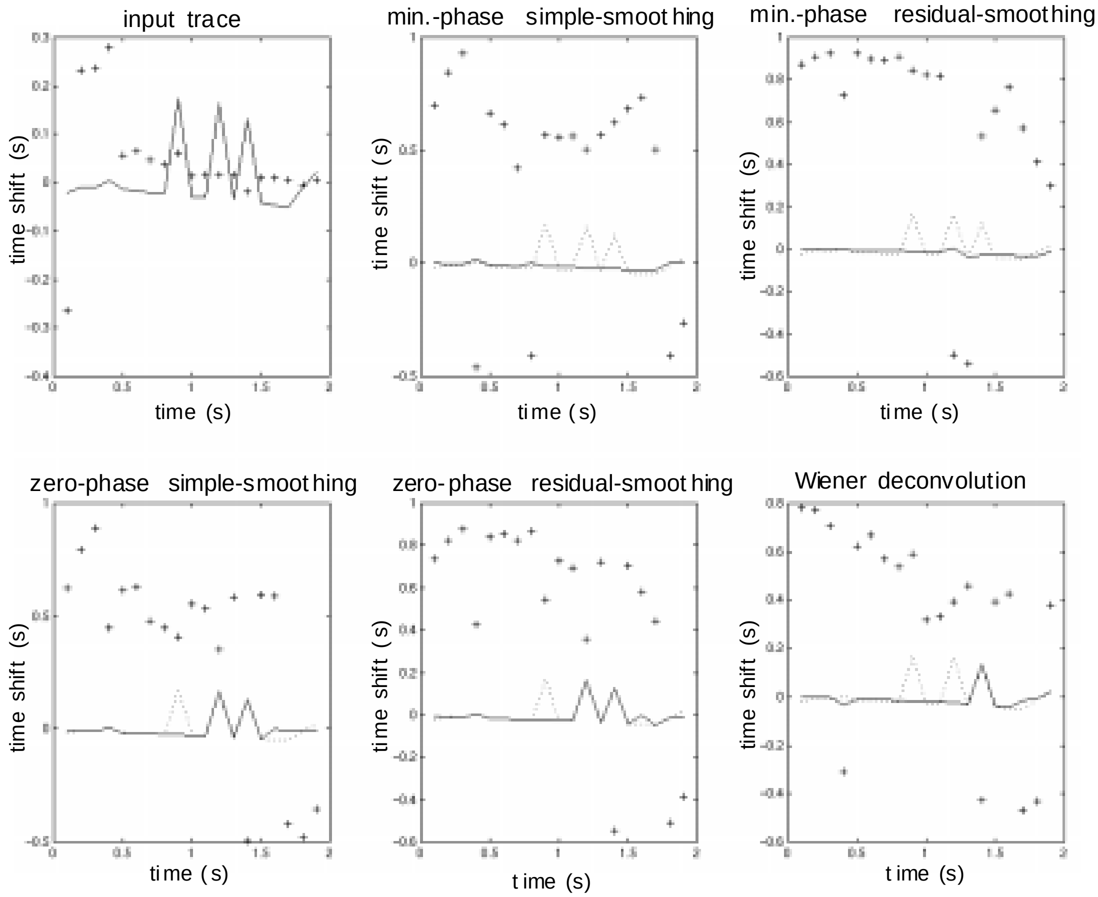

Figure 8: A comparison of the time shift of events for zero and minimum-phase residual-smoothing methods, simple-smoothing methods and gain and Wiener deconvolution. Segments of the traces (0.2 seconds in length) were correlated to corresponding segments of the bandlimited reflectivity. The solid line shows the time shift associated with the maximum correlation of the deconvolution method and the dotted line shows the time shift associated with the maximum correlation of the input trace. The '+' symbol indicates the values of the maximum correlation at the corresponding time. The value of the maximum correlation value can be read off the y-axis, however it has no physical units. A positive shift in time indicates that events has been advanced in relation to the bandlimited reflectivity. The value of the maximum correlation indicates how strongly the trace correlated with the bandlimited reflectivity.

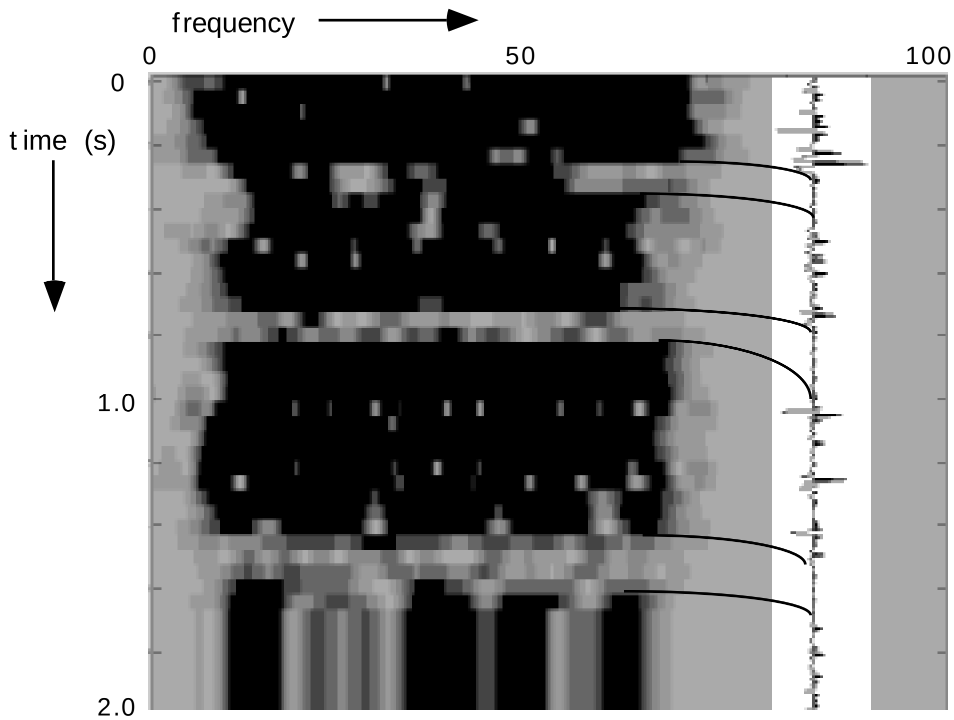

Figure 9: The bands in the |TVS| of the bandlimited reflectivity correspond to features in the trace.

As can be seen from figure 5, the output traces from all versions of TVSI show an increase in amplitude of events at later times as compared to the input trace. In addition to the amplitude corrections, the |TVS| of the output traces from TVSI (figure 6) also show that much of the bandwidth at later times has been recovered. The residual-smoothing process seems more effective than simple-smoothing and, as can be seen from figure 5, its output seems to match the reflectivity better than the result from simple-smoothing. The improvement in performance of the residual-smoothing method over the simple-smoothing method is related directly to the removal of the exponential attenuation surface before smoothing.

We have found that deconvolution based on the zero-phase residual-smoothing version of TVSI yields results similar to that of TVSW, as can be seen in figure 5. The last two traces of figure 5 are a result of a combination of gain and Wiener deconvolution and gain and stationary frequency domain deconvolution. Both of these traces still exhibit reflections which broaden in time, indicating that the effects of attenuation have not been fully removed. The |TVS| of both combinations of gain and stationary deconvolution (figure 7) exhibit a strong loss of bandwidth with time.

The minimum-phase output in both versions of TVSI are more favorable than the zero-phase outputs. The minimum-phase option helps to reduce the time shift of events in the input trace. This time shift is associated with dispersion and the embedded minimum-phase wavelet. The advantage of the minimum-phase results over the zero-phase results are particularly obvious in the |TVS| of figure 6. The light-colored band on the |TVS| of the bandlimited reflectivity at approximately 0.8 seconds is linear and corresponds to features in the trace, as is shown in figure 9. The |TVS| of the input trace has a corresponding light-colored band, however between 0 and 30 Hz the band occurs at a slightly later time than on the bandlimited reflectivity and it is difficult to discern after 30 Hz. The |TVS| of the minimum-phase results show that the light colored band is linear and at approximately the same time as the band on the |TVS| of the reflectivity. The |TVS| of the zero-phase results shows a shift in the band at approximately 30 Hz. The position of the band between 0 and 30 Hz corresponds to the position of the section of the band which is visible on the |TVS| of the input trace. This shift in the band could be due to dispersion present in the input trace which is not corrected by the zero-phase operator. The linear feature occurs at approximately 0.8 seconds in the |TVS| of the gain and Wiener deconvolution, gain and stationary frequency domain deconvolution, and TVSW. It is not strong and continuous like the band on the bandlimited reflectivity.

Although each row of the 'zero-phase' operator is zero phase, such operators will generally change both the amplitude and phase of a trace when applied through equation (9). For more information, refer to Margrave (1997).

Figure 8 plots the maximum correlation and associated time shifts between segments of a particular output trace and the bandlimited reflectivity. The segments were 0.2 seconds in length and overlapped each other by 0.1 seconds. As expected, the input trace has a time advancement due to dispersion and the embedded minimum-phase wavelet. The maximum correlation values are low indicating a poor match between the input trace and the bandlimited reflectivity. A combination of gain and Wiener deconvolution has reduced these shifts, particularly in the early part of the trace. The maximum correlation values decrease with time indicating that the operator could not correct for the nonstationarity of the input trace. The zero-phase TVSI methods have slightly changed the phase of the input trace, for reasons discussed above. Both minimum-phase TVSI methods have produced a reasonable correction of the time shift and the corresponding maximum correlation values are relatively high.

TVSI asks for several parameter inputs from the user. The user-specified parameters that affect the results most significantly are the length of the frequency and time smoothers. Figures 10 to 15 shows how the smoother length influences the results of minimum-phase simple-smoothing and minimum-phase residual-smoothing.

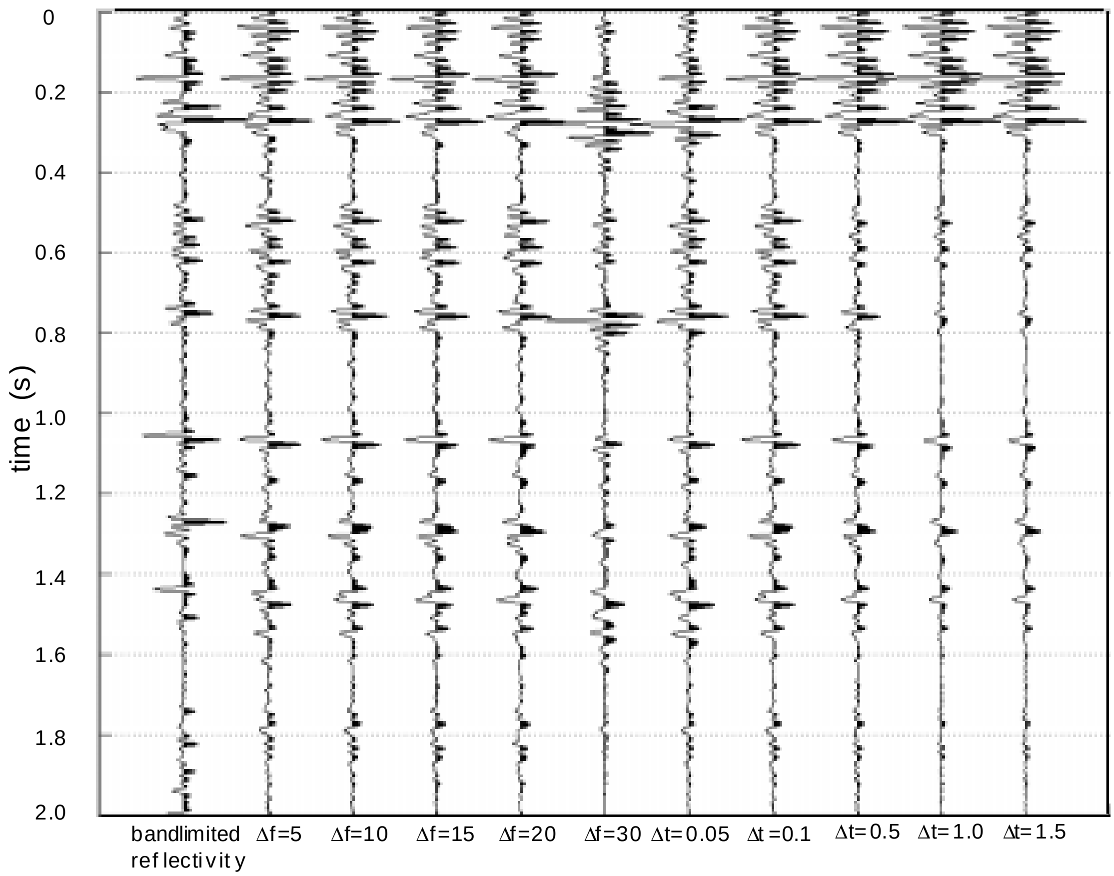

Figure 10: The length of the time and frequency smoothers were varied to determine how they affected the output from the minimum-phase simple-smoothing version of TVSI. The length of the time smoother was held constant at 0.5 seconds while the length of the frequency smoother, Δf, was changed from 5 to 30 Hz. The length of the frequency smoother was held constant at 10 Hz while the length of the time smoother, Δt, was varied from 0.05 to 1.5 seconds.

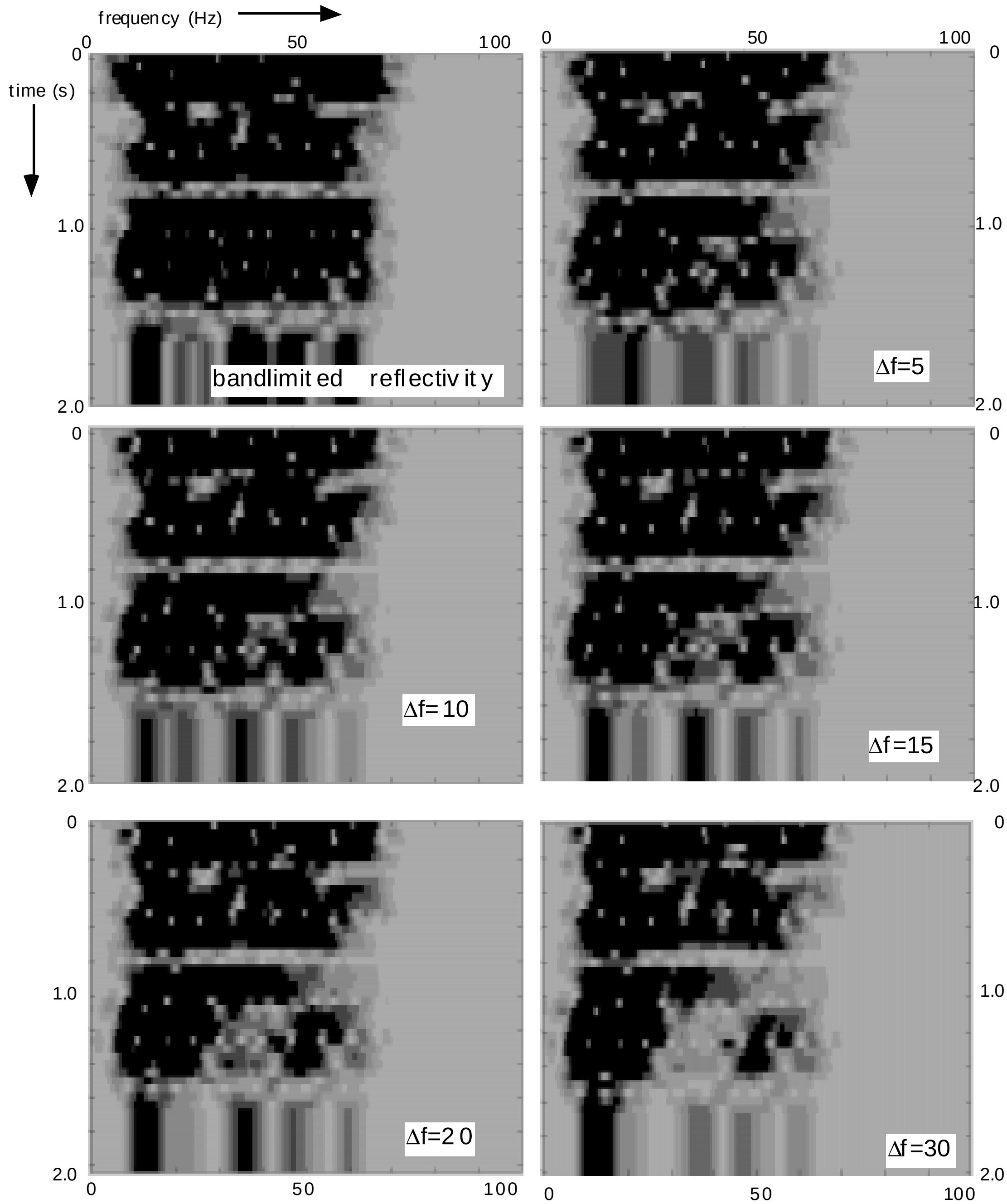

Figure 11: The |TVS| of the resultant traces from the frequency smoother tests of the minimum-phase simple-smoothing method. The length of the time smoother was held constant at 0.5 seconds.

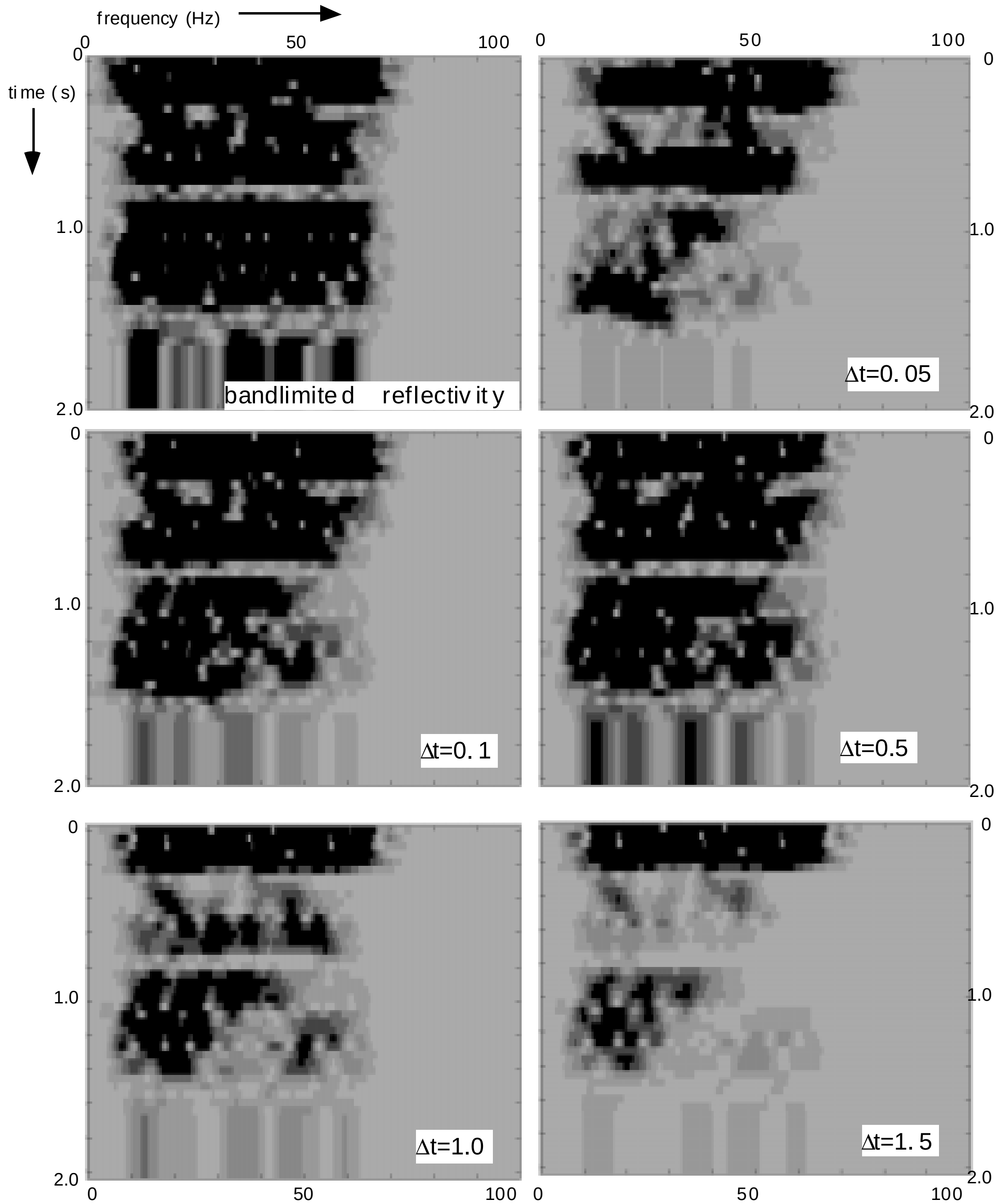

Figure 12: The |TVS| of the resultant traces from the time smoother tests of the minimum-phase simple-smoothing method. The frequency smoother was held constant at a length of 10 Hz.

The simple-smoothing method of TVSI seems to performs best when used with small time and frequency smoothers. Long smoothers bias the exponential attenuation surface and distort the operator. The |TVS| displayed in figure 11 and 12 show how the high frequencies are lost, especially at later times, with longer time and frequency smoothers. From equation 4, we can see that the length of the frequency smoother in the frequency domain is inversely proportional to its length in the time domain. The frequency smoother therefore must be small enough to allow its time-domain equivalent to encompass the majority of the wavelet. The wavelet is commonly about 0.2 seconds in length, so a 5 Hz smoother would completely encompass it. Therefore, a frequency smoother of length 10 Hz and a time smoother of length 0.5 seconds seems reasonable.

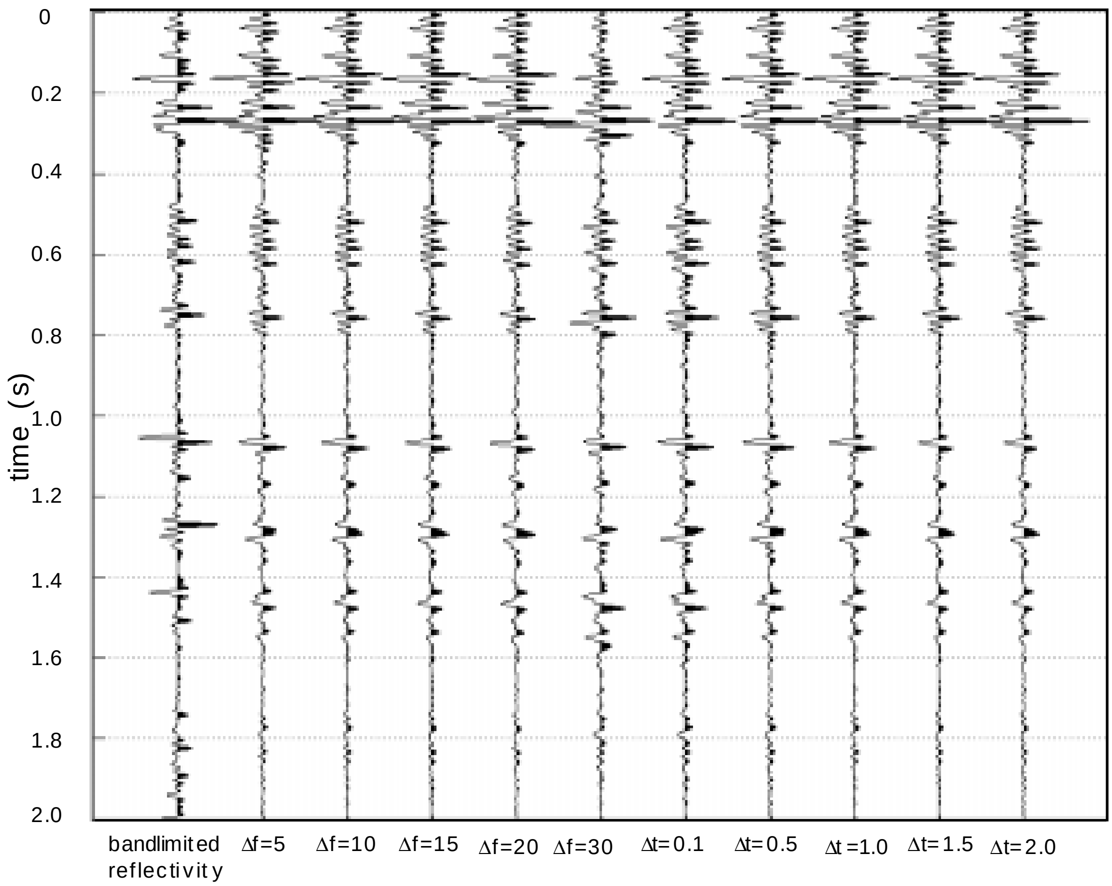

Figure 13: The length of the time and frequency smoothers were varied to determine how they affected the output from the minimum-phase residual-smoothing version of TVSI. The length of the time smoother was held constant at 1.5 seconds while the length of the frequency smoother, Δf, was changed from 5 to 30 Hz. The length of the frequency smoother was held constant at 10 Hz while the length of the time smoother, Δt, was varied from 0.1 to 2.0 seconds.

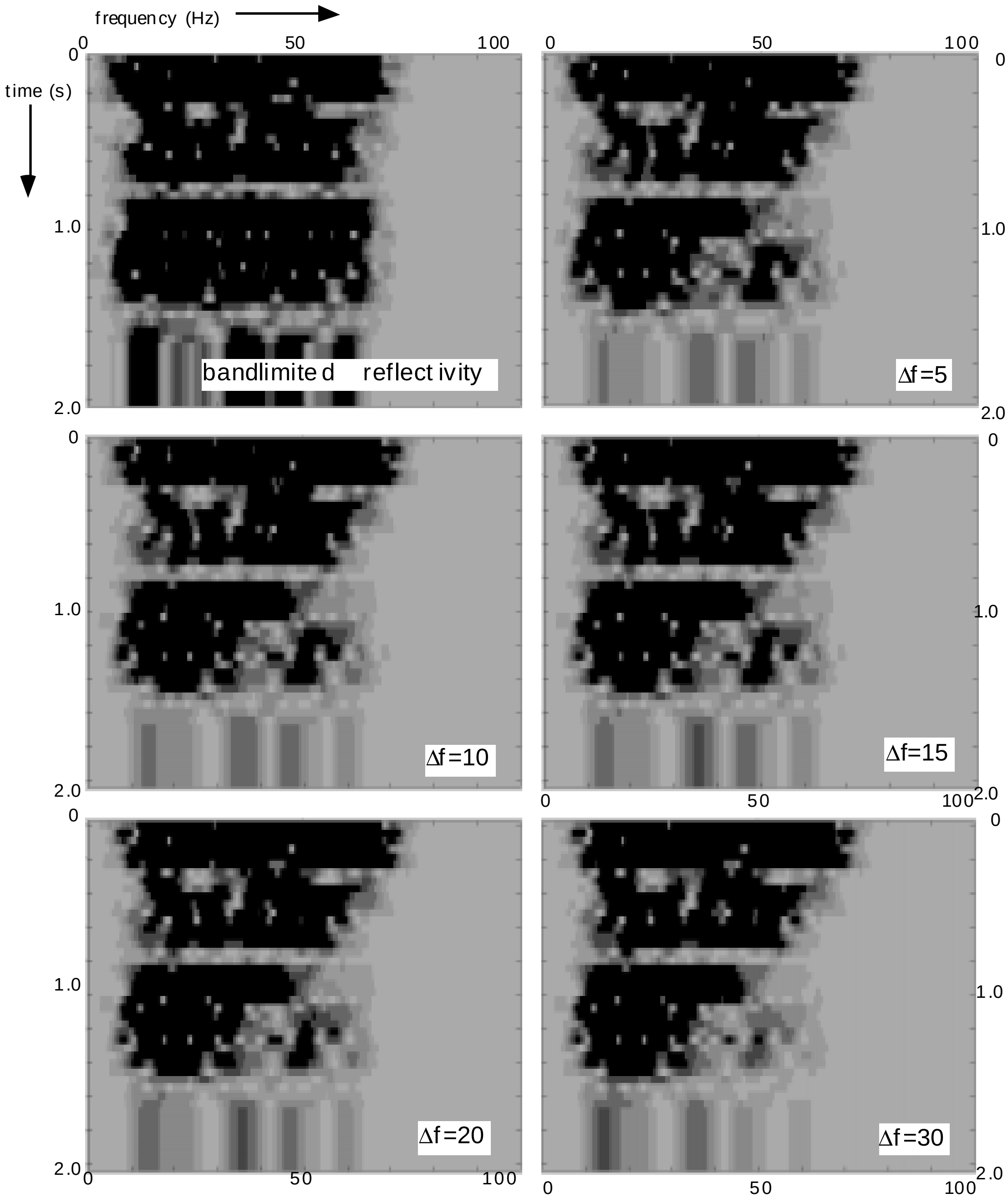

Figure 14: The |TVS| of the output traces from the frequency smoother tests for the minimum-phase residual-smoothing method. The length of the time smoother was held constant at 1.5 seconds.

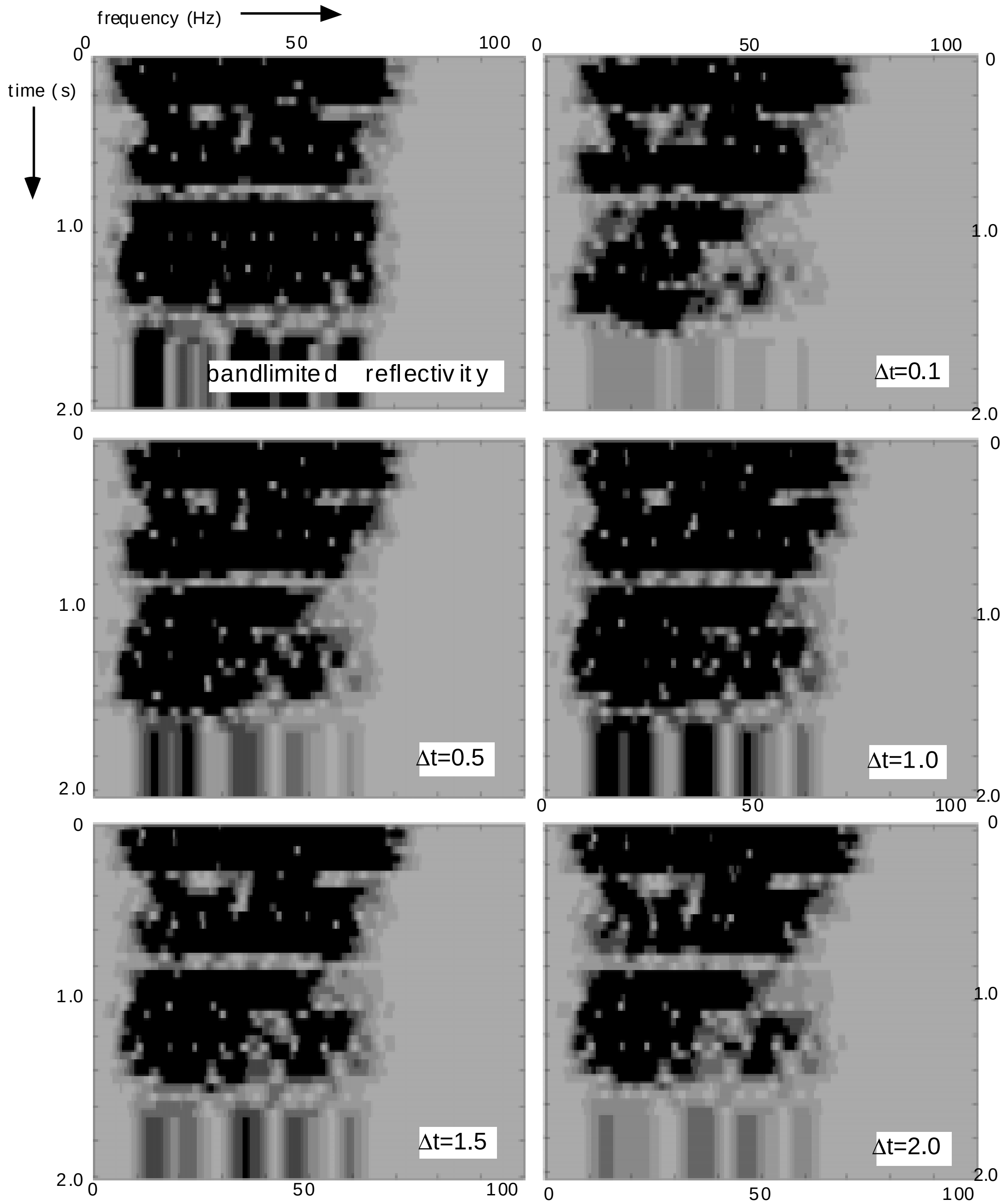

15: The |TVS| of the output traces from the time smoother tests for the minimum-phase residual-smoothing method. The length of the frequency smoother was held constant at 10 Hz.

Based on the traces of figures 13 and the |TVS| in figures 14 and 15, a long time smoother and a short frequency smoother seem reasonable for the minimum-phase residual-smoothing method. The residual-smoothing method models the residual spectrum to be smoothed, as only containing the source waveform and reflectivity. The source waveform is stationary in time, however it is frequency dependent. Therefore, time smoothers should not adversely affect the spectrum of the source waveform. However, the frequency smoothers should be kept short, so as not to distort this spectrum. As with the simple-smoothing method, the frequency smoothers must be short enough in the frequency domain that they will be long enough to encompass the entire wavelet in the time domain.

The TVSI operator is determined from the data and not designed explicitly from a value of Q. The Q estimate is only used to remove an approximate attenuation surface to form the residual spectrum, and this attenuation surface is replaced after the residual spectrum has been smoothed. This suggests that TVSI may be relatively insensitive to errors in the estimate of Q. Q is difficult to estimate in practice, and being able to remove attenuation without an exact value of Q would be advantageous. A noise-free and multiple-free synthetic trace has been attenuated with a Q of 100. This trace has been input into TVSI with varying erroneous values of Q, as well as the correct value, to determine how accurate a Q estimate must be to filter the trace satisfactorily.

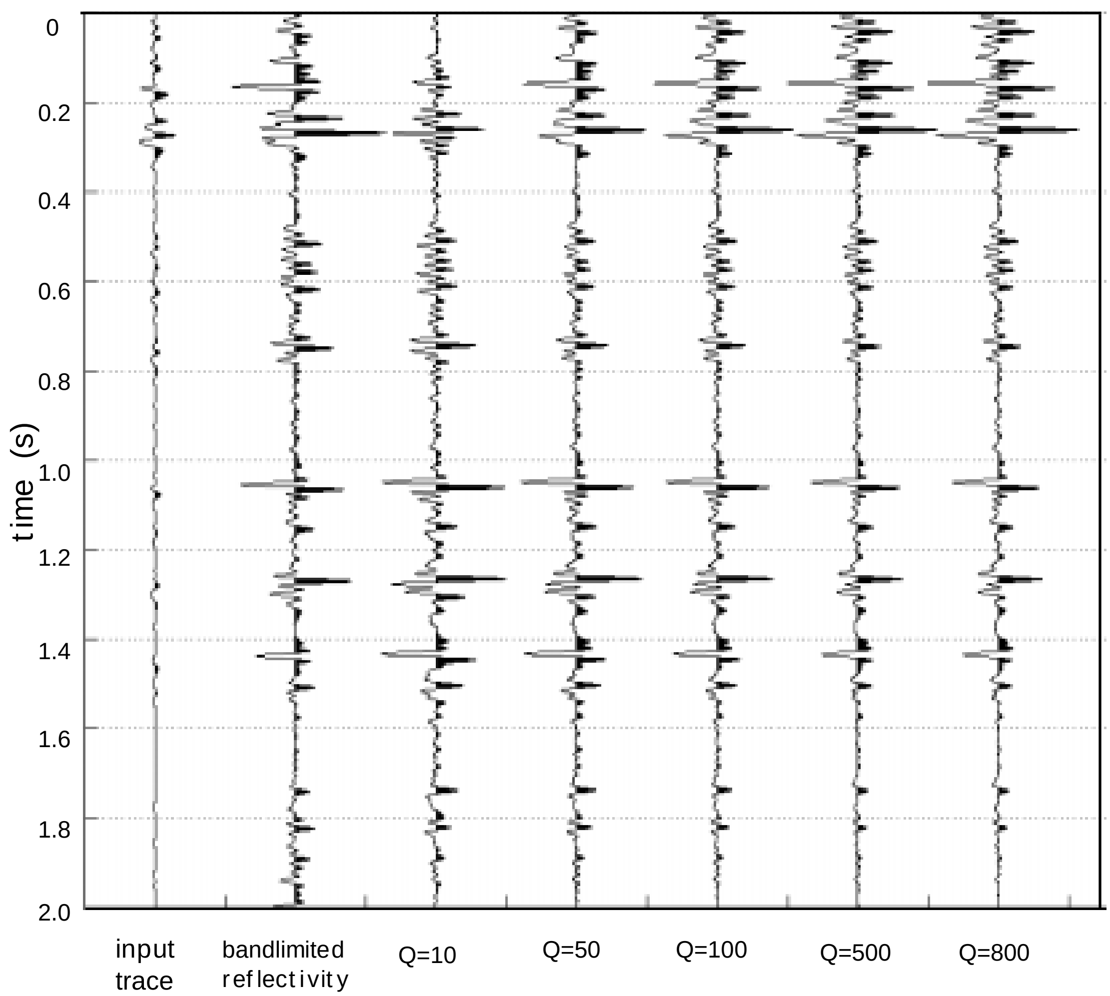

Figure 16: The minimum-phase residual-smoothing method was tested for its sensitivity to errors in the value of Q. The input trace was created with a Q value of 100. Then the trace was deconvolved with minimum-phase residual-smoothing TVSI using various values of Q.

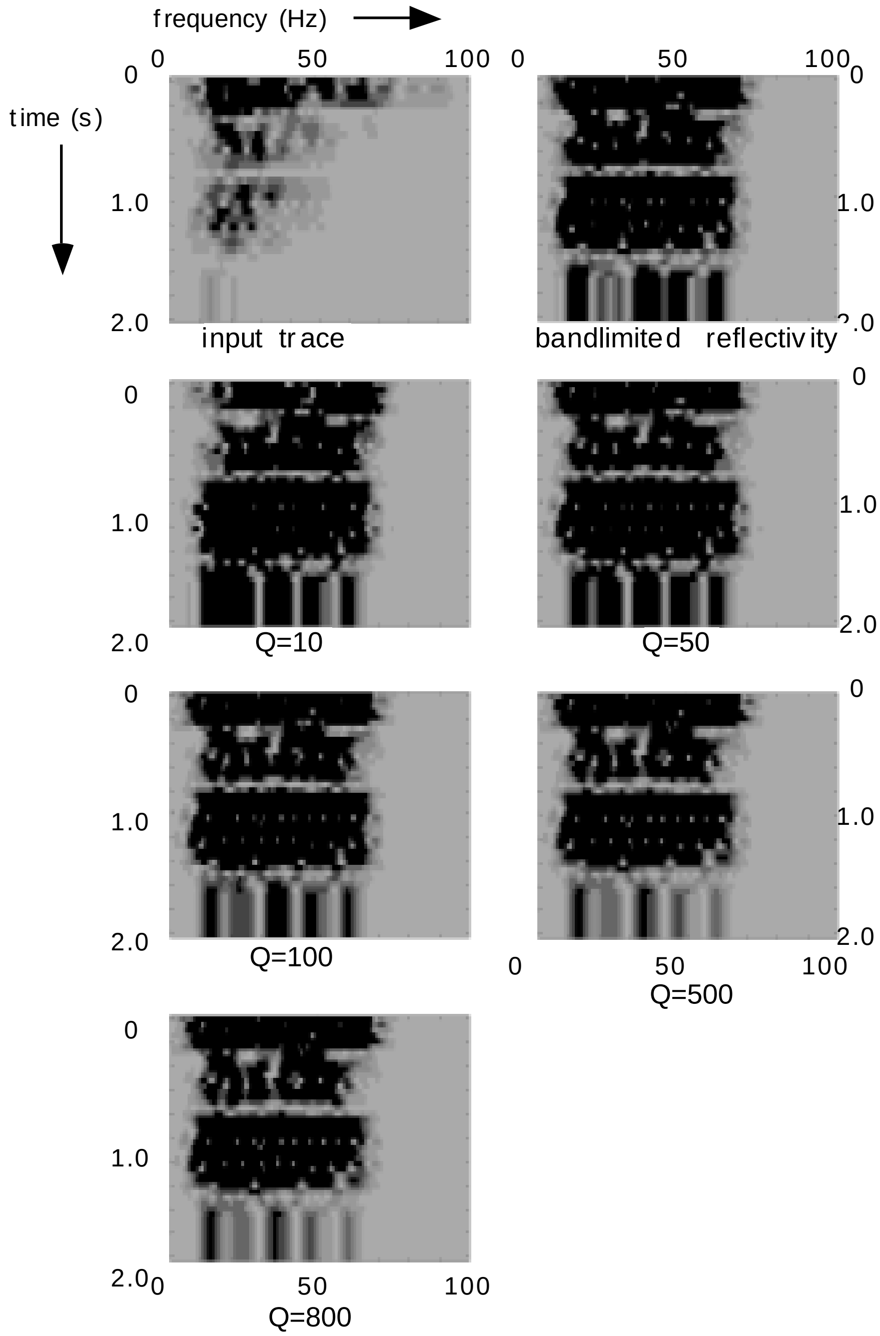

Figure 17: The |TVS| of the output traces from the Q-sensitivity tests in the minimum-phase residual-smoothing method.

Estimating Q to be of a higher value than it actually is, still yields reasonable results from TVSI (figures 16 and 17). The attenuation surface is not entirely removed before smoothing when the Q estimate is higher than the actual value. The extreme case of this would be not removing any part of the attenuation surface which is analogous to the simple-smoothing version. TVSI is also forgiving about estimating Q to be lower than the actual value. Errors in the estimate of Q will commonly fall within the range of Q values that the TVSI algorithm is relatively insensitive towards.

CONCLUSIONS

A nonstationary Fourier-domain deconvolution routine, TVSI, has been developed as an extension of stationary Fourier domain deconvolution. It uses a data-dependent operator derived from the time-variant amplitude spectrum of the input trace to approximately correct for the effects of attenuation, dispersion, multiple effects and source signature. Two versions of the deconvolution method are available, and they differ in the way the nonstationary spectrum of the input data is smoothed in the operator design stage. The first version, the simple-smoothing method, directly smoothes the |TVS| of the input trace. It yields a result similar to that of time-variant spectral whitening (TVSW), however with two differences. The operator can be minimum phase. The alternate version, the residual-smoothing method, is a type of data-driven inverse-Q filter. The residual-smoothing process removes an estimated exponential attenuation trend from the time variant amplitude spectrum of the input trace, smoothes the residual spectrum and restores the exponential attenuation trend. The resulting amplitude spectrum, from either version, can then be coupled with a minimum-phase spectrum or left as zero phase before being inverted to form the inverse operator. The inverse operator is then applied to the trace using nonstationary filtering techniques. TVSI has an advantage over other inverse-Q filtering techniques. It seems to be robust with respect to the estimate of Q and the operator is continuously time variant. As well, TVSI can also handle waveform removal and certain classes of multiples.

ACKNOWLEDGEMENTS

We wish to thank the sponsors of the CREWES project for their support of this research.

REFERENCES

Aki, K., and Richards, P. G., 1980, Quantitative Seismology Theory and Methods, W. H. Freeman and Company.

Bickel, S. H. and Natarajan, R.R., 1985, Plane Wave Deconvolution: Geophysics, **50**, 1426-1439

Cohen, L., 1995, Time-Frequency Analysis: Prentice Hall

Futterman, W. I, 1962, Dispersive Body Waves: Journal of Geophysical Research, **73,** 3917-3935

Gelius, L.J., 1987, Inverse Q filtering. A spectral balancing technique: Geophysical Prospecting, **35**, 656-667

Hale, D., 1982, Q adaptive deconvolution: Stanford Exploration Project, **30**, 133-158

Hargreaves, N. D., 1992, Similarity and the inverse Q filter: some simple algorithms for inverse Q filtering: Geophysics, **57**, 944-947

Johnston, D. H., and Toksov, M. N., 1981, Seismic Wave Attenuation: Geophysics Reprint Series No. 2, Society of Exploration Geophysics

Karl, J. H., 1989, An introduction to Digital Signal Processing, Academic Press

Kjartannson, E., 1979, Constant Q wave propagation and attenuation: J. Geophys. Res., **84**, 4737-4748

Margrave, G. F., 1997, Nonstationary Linear Filter Theory: Review and Update: 9th Annual CREWES Research Report

Margrave, G.F., 1998, Theory of nonstationary linear filtering in the Fourier domain with appllication to time variant filtering: in press Geophysics and 1996 CREWES meeting

Schoenberger, M., and Levin, F. K., 1974, Apparent Attenuation Due to Intrabed Multiples: Geophysics, **39**, 278-291

Yilmaz, O., 1987, Seismic Data Processing, Society of Exploration Geophysicists